American Mineralogist, Volume 87, pages 262–268, 2002

X-ray spectroscopic investigations of fluids in the hydrothermal diamond anvil cell: The hydration structure of aqueous La^{3+} up to 300 °C and 1600 bars

ALAN J. ANDERSON,[1,*] SUMEDHA JAYANETTI,[2,†] ROBERT A. MAYANOVIC,[2] WILLIAM A. BASSETT,[3] AND I-MING CHOU[4]

[1]Department of Geology, St. Francis Xavier University, Antigonish, Nova Scotia, B2G 2W5, Canada
[2]Department of Physics and Astronomy, Southwest Missouri State University, Springfield, Missouri 65804, U.S.A.
[3]Department of Geological Sciences, Cornell University, Ithaca, New York 14853, U.S.A.
[4]MS 954, U.S. Geological Survey, Reston, Virginia 20192, U.S.A.

ABSTRACT

The first direct measurements are reported for the structure of the hydrated La^{3+} ion in an aqueous solution (containing 0.007 *m* La) over a range of temperatures from 25 to 300 °C and pressures up to 1600 bars. The radial distribution of atoms around the La^{3+} ion was measured using the X-ray absorption fine structure (XAFS) technique. La L_3-edge spectra were collected in the fluorescence mode from nitrate solutions in a modified hydrothermal diamond anvil cell using the PNC-CAT X-ray microprobe at the Advanced Photon Source, Argonne National Laboratory. Analysis of the XAFS spectra collected at all temperatures indicates that each La^{3+} ion has a hydration number of nine and that the solvating waters surround the ion in a tricapped trigonal prismatic arrangement. As temperature is increased from 25 to 300 °C, the bond distance between the equatorial-plane O atoms and the La^{3+} ion increases from 2.59 ± 0.02 to 2.79 ± 0.04 Å, whereas the bond distance between La^{3+} and the O atoms at the ends of the prism decrease to 2.48 ± 0.03 Å. This study also demonstrates the unique capability of the modified hydrothermal diamond anvil cell for in situ low energy X-ray spectroscopic analysis of elements in dilute aqueous solutions at elevated temperatures and pressures.

INTRODUCTION

In the past decade many theoretical and experimental studies have contributed to our understanding of the mobility of rare earth elements (REEs) in the hydrosphere (e.g., Wood 1990; Haas et al. 1995; Lewis et al. 1998; Gammons and Wood 2000). The special attention given to the aqueous geochemistry of the REEs stems from their importance as tracers in a variety of geochemical processes (Brookins 1989; Henderson 1985), the need to understand the genesis and chemical controls of REE hydrothermal ore deposition (Taylor and Fryer 1982; Williams-Jones et al. 2000), and the use of the REE group as an analogue in studying the behavior of elements of the similar actinide group (Krauskopf 1986).

Although significant progress has been made in calculating REE speciation in aqueous solutions, very little is directly known about the structure, stoichiometry, and stability of REE complexes in hydrothermal systems. Habenschuss and Spedding (1979a, 1979b) studied the hydration of rare earth ions in aqueous chloride solutions at ambient conditions by X-ray diffraction. Photoacoustic spectroscopy (PAS) has been used to provide direct information on REE species in sparingly soluble systems under ambient conditions (Wood et al. 1995). Ragnarsdottir et al. (1998) investigated the local structure of yttrium in 0.1 *M* YCl_3-bearing aqueous solutions from 25 to 340 °C using extended X-ray absorption fine structure spectroscopy. However, there are presently no direct measurements of REE complexes at elevated temperatures and pressures in aqueous solutions having low concentrations typical of natural hydrothermal systems.

In this study the hydration structure of La^{3+} in aqueous nitrate solutions (containing 0.007 *m* La) from 25 to 300 °C is investigated in a hydrothermal diamond anvil cell designed specifically for XAFS analysis in the fluorescence mode. The new hydrothermal diamond anvil cell has a shallow sample chamber and grooves cut into the face of one of the diamond anvils. This cell has the advantage of extending analytical capabilities to micromolar concentrations of elements having X-ray absorption edge energies as low as 5000 eV up to temperatures of 700 °C and several kilobars of pressure thus making it possible to study K-edge absorption spectra of relatively low *Z* elements such as V or Ti and L-edge absorption of the light REEs in fluids at extreme conditions. The advent of bright third generation synchrotron sources has made these difficult experiments possible.

Measurements at different pressures and temperatures with the diamond anvil cell are conducted on a fluid of constant density (i.e., isochoric). The trajectory of the isochore in pressure-temperature space can be controlled by adjusting the density of the fluid after loading. This is done by controlled leakage of the fluid at 110 °C followed by rapid sealing of the cell. In the present study the density of the fluid was set at 870 kg/m^3. Previous work has shown that temperature, rather than pres-

* E-mail: aanderso@stfx.ca
† On leave from the Department of Physics, University of Colombo, Sri Lanka.

sure, is the dominant factor affecting aqua ion stability in a pressure range of less than about 2 or 3 kbars (Seward and Barnes 1997). Therefore additional measurements at various pressures, involving the difficult operation of reloading the cell with a solution of a different density, were unnecessary.

Direct measurements of the solvation of the rare earth elements in hydrothermal solutions are needed to validate the theoretical models used for thermodynamic predictions. The results presented here on aqueous La^{3+} also serve as an important starting point for future XAFS investigations of REE association with ligands such as Cl^-, F^-, OH^-, CO_3^{2-}, and PO_4^{3-}.

XAFS ANALYSIS AT ELEVATED TEMPERATURES AND PRESSURES

Direct determination of the structural properties of aqueous ions from near ambient conditions up to high-grade metamorphic temperatures and pressures is of considerable interest to geochemists studying fluid-related processes in the Earth's crust. In recent years, a number of high temperature cells have been constructed for the purpose of X-ray absorption spectroscopic analysis of ions in hydrothermal solutions (e.g., Anderson et al. 2000; Bassett et al. 2000a; Fulton et al. 1996; Seward et al. 1999). An important feature in the design of these cells is the X-ray window, which must be strong enough to withstand high internal pressure, yet thin enough to effectively transmit the photon energies of interest. Sealed capillaries with 1 to 2 mm thick silica-glass walls have been used for high temperature XAFS measurements to 350 °C and at equilibrium vapor pressures (e.g., Mosselmans et al. 1996; Oelkers et al. 1998; Ragnarsdottir et al. 1998; Sherman et al. 2000). Fulton et al. (1996) and Hoffmann et al. (2000) extended the conditions of XAFS measurements for hydrothermal solutions to 425 °C and 600 bars by using an internally Pt plated nickel alloy and thick diamond windows. However, attenuation by thick glass walls or diamond windows precludes the analysis of elements having X-ray absorption energies less than about 6000 eV.

Mayanovic et al. (1999) and Anderson et al. (2000) measured XAFS spectra in the transmission mode from zinc halide solutions up to 660 °C and 8.0 kbar using a hydrothermal diamond anvil cell. The cell was modified to provide enhanced transmission of X-rays by laser drilling tunnels in both diamonds to within 150 μm of the anvil faces. This design significantly extends the pressure and temperature limits of XAFS analysis; however, spectral acquisition in the transmission mode lacks the sensitivity for analysis of trace concentrations in solution.

All XAFS spectra reported in this paper were collected in the fluorescence mode from solutions in a modified hydrothermal diamond anvil cell (Bassett et al. 2000b). The solution was sealed between the upper and lower diamond anvils in a sample chamber consisting of a 300 μm diameter cup-shaped cavity in the center of the upper diamond anvil face and a 300 μm diameter hole in a 50 μm thick Re gasket (Fig. 1). The solution was irradiated by an X-ray beam that traveled through the upper diamond in a direction parallel to the anvil face. A laser-milled groove in the face of the upper diamond anvil reduced the path length of the incident beam through the diamond. A second groove, oriented at 90° to the direction of the incident X-ray beam, was milled to within 80 μm of the solution chamber in order to minimize the attenuation of fluorescence X-rays impinging upon the detector. Figure 2 illustrates the enhanced transmission of X-rays in the modified hydrothermal diamond cell relative to other cell windows used in previous XAFS studies of hydrothermal solutions.

EXPERIMENTAL METHODS

Spectral acquisition

A 0.007 *m* La (2% HNO_3) standard solution was loaded in the sample chamber of a hydrothermal diamond anvil cell having grooves drilled into the upper diamond anvil (Fig. 1b). La L_3-edge (5483 eV) XAFS spectra were collected on the undulator PNC-CAT ID20 beam line, at the APS. The spectra were collected in fluorescence mode, in the standard horizontal 90° orientation to the incident X-ray beam using a 13-element Ge detector. The synchrotron was operated at 7.0 GeV and 100 mA maximum fill current. Energy calibration was accomplished using vanadium foil (K edge = 5465 eV). The crystals of the monochromator were detuned by 30–40% in order to reduce the harmonic content in the incident X-ray beam. Each of the spectra were collected for 20 minutes and up to six such scans were repeated at each temperature.

Analysis of XAFS data

The XAFS spectrum for each scan was obtained by the averaging of the signal collected from the individual fully functioning channels of the 13-element Ge detector. For a given temperature, the XAFS spectra were further refined by the averaging up to two or three separate scans out of six scans. Only those scans having suitably high signal-to-noise ratio were selected for the data analysis. Variations in signal-to-noise characteristics were caused by spurious electronic noise in the 13-element Ge detectors. For temperatures up to 255 °C, the XAFS spectra shown in Figure 3 were obtained by averaging three such scans. In order to minimize some of the noise from the XAFS signal in the energy range E > 5600 eV (or > 5.5 $Å^{-1}$ in k-space) two-point averaging was used. The spectrum at 300 °C was obtained by averaging only two scans. Due to the low signal to noise ratio of the data at 300 °C, noise minimization was achieved by employing one-point smoothing throughout the XAFS range.

Solera et al. (1995) recognized an anomalous feature in the region of 5600 eV, which they attribute to multi-electron transitions. This feature was identified and removed from our data prior to background removal. Data were then normalized with respect to the intensity of the incident beam. XAFS oscillations, $\chi(k)$, were extracted using an automated background subtraction program (AUTOBK) developed by Newville et al. (1993). Figure 4 shows the k^2 weighted $\chi(k)$ data, with the multi-electron excitation feature in the region of 5.4–5.9 $Å^{-1}$ removed from each temperature-dependant spectrum.

The data analyses were done using the FEFFIT2.54 software program (Newville et al. 1995; Stern et al. 1995) that employs a nonlinear, least square fit to the theoretical standards calculated using FEFF8 theoretical code (Zabinsky et al. 1995). Several factors were taken into account in choosing the

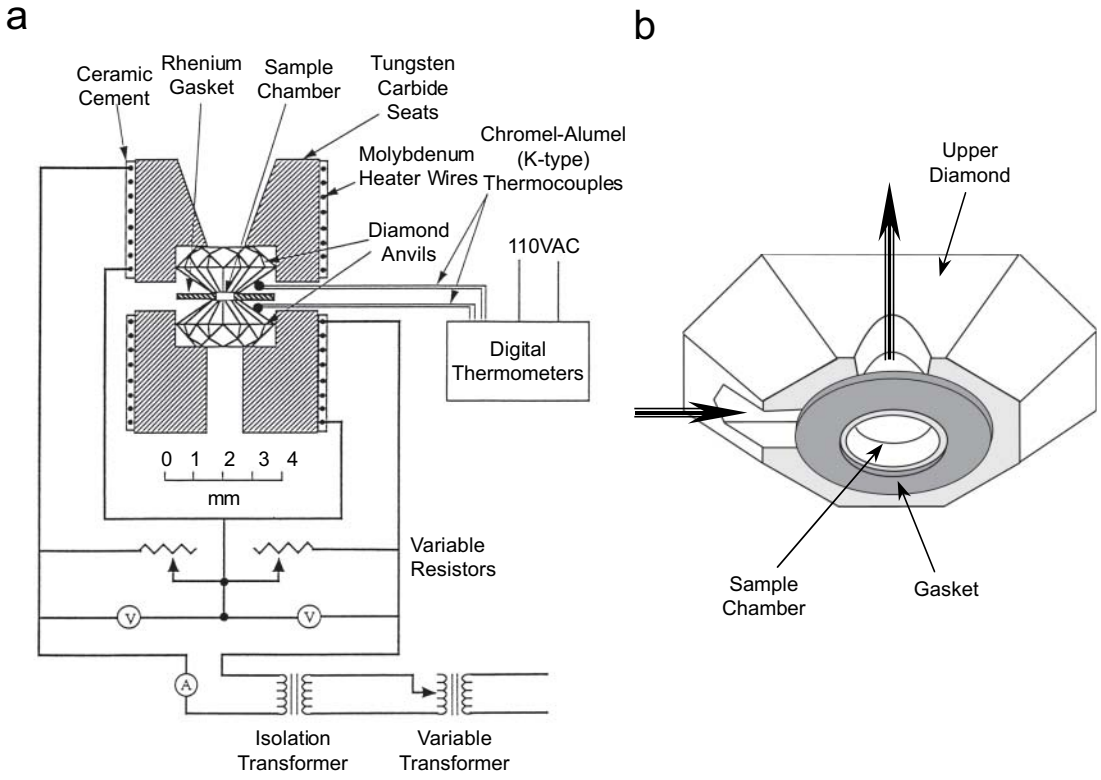

FIGURE 1. (**a**) A schematic diagram of a Bassett-type hydrothermal diamond anvil cell (HDAC). (**b**) The schematic diagram of the upper diamond of the modified HDAC showing the entrance and exit grooves for the incident and fluorescence X-rays, respectively. The laser drilled sample chamber is located in the center of the upper diamond anvil face above the hole in the gasket.

appropriate k^n weighting for analysis of the $\chi(k)$ spectra. The range of each $\chi(k)$ spectrum that is available for analysis is limited to about 10.0 $Å^{-1}$ due to the occurrence of the La L_2-edge at 5891.0 eV. In addition, the presence of the noise, and the weak back-scattering nature of oxygen near neighbors in the high k region, makes k^1 or k^2 weighting more suitable than k^3 weighting for analysis of $\chi(k)$ data (Sayers and Bunker 1998). Thus, the $\chi(k)$ data were weighted by k^2 and fit in the k-ranges given in Table 1, using a Hanning window with dk = 1.0 $Å^{-1}$. Fitting parameters included the coordination number (N), the radial distance (R), the XAFS Debye-Waller factor (σ^2) and ΔE_0 that adjusts for the mismatch between the experimental edge energy and its theoretical estimate. First, during the fitting of the room-temperature data, ΔE_0 was allowed to vary freely with other fitting parameters. It was then fixed at the same value for fitting of data collected at other temperatures. The amplitude reduction factor, $S_0^2 = 0.94$, obtained from Haskel et al. (2000) and Ankudinov (personal communication) was used during fitting. The $\Re$-factor given in Table 1 is a measure of the quality of the fit. In general, this factor is <0.05 for a good fit.

Fitting of the room temperature and 100 °C data was initially done in both R-space and back transformed k-space of data filtered in the R-range of 1.0–3.0 Å using a single shell model. When all the fitting parameters were allowed to vary

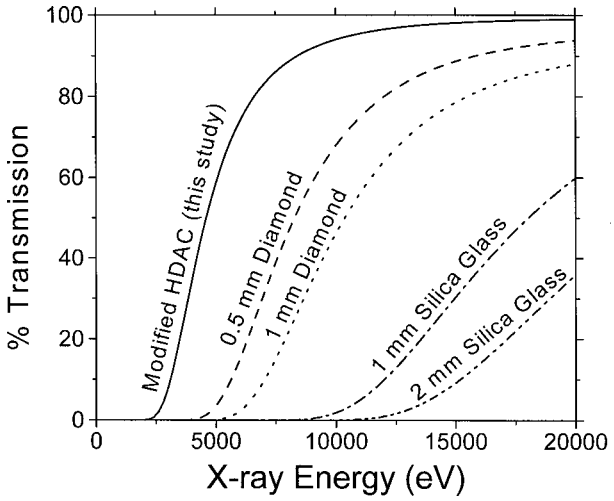

FIGURE 2. Percent transmission of X-rays as a function of energy through windows of various thickness and composition used in previous XAFS studies of hydrothermal solutions compared to the modified HDAC.

TABLE 1. Fitting results for XAFS spectra measured from La (0.007 *m*) in nitrate solution

Temp.	k-range (Å^{-1})	R-range (Å)	N_O†	$R_{La\text{-}O}$ (Å)	$\sigma^2_{La\text{-}O}$ (Å^2)	ΔE_0 (eV)	ℜ-factor
RT	2.0–8.2	1.0–3.0	8.3 ± 1.0	2.59 ± 0.02	0.009 ± 0.003	6.66	0.022
(s.s. fit)		(1.4–3.0)	(8.0 ± 1.0)	(2.59 ± 0.01)	(0.008 ± 0.003)	(6.78)	(0.013)
100 °C	2.0–8.2	1.0–3.0	8.1 ± 0.6	2.60 ± 0.02	0.017*	6.70*	0.038
(s.s. fit)		(1.4–3.0)	(8.0 ± 0.5)	(2.60 ± 0.02)	(0.017*)	(6.70*)	(0.021)
255 °C	2.0–8.6	1.4–3.0	5.4 ± 1.3	2.46 ± 0.02	0.008 ± 0.005	6.70*	0.014
(d.s. fit)			3.7 ± 0.7	2.71 ± 0.0	0.008 ± 0.005		
300°C	2.0–8.6	1.0–3.0	5.7 ± 0.9	2.48 ± 0.02	0.008*	6.70*	0.069
(d.s.fit)			2.9 ± 1.1	2.79 ± 0.06	0.010*		
		(1.4–3.0)	(5.7 ± 0.6)	(2.48 ± 0.02)	(0.008*)	(6.70*)	(0.028)
			(2.8 ± 0.9)	(2.79 ± 0.04)	(0.010*)		

Note: The fitting parameters within parentheses corresponding to the filtering range 1.4–3.0 Å lead to smaller ℜ-factors for fits obtained at 25, 100, and 300 °C.
* $\sigma^2_{La\text{-}O}$ and ΔE_0 were constrained at these values during fitting.
† The coordination numbers were determined using $S_0^2 = 0.94$ that was obtained from Haskel et al. (2000) and Ankudinov (personal communication).

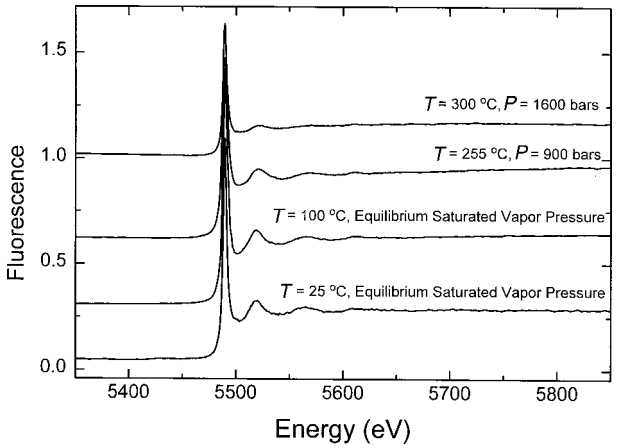

FIGURE 3. La L_3-edge XAFS spectra collected in the fluorescence mode from a 0.007 *m* La aqueous solution at temperature ranging from 25 to 300 °C.

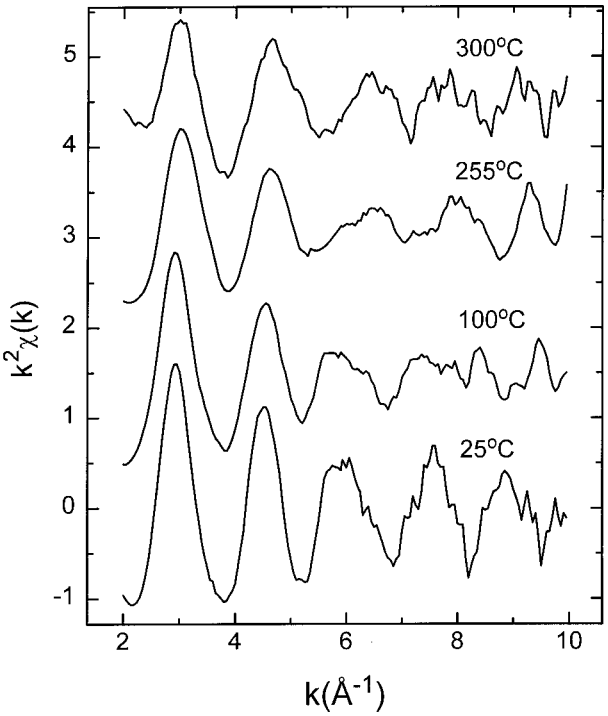

FIGURE 4. XAFS ($k^2\chi$) data as a function of temperature after removal of the multi-electron excitation feature in the region around 5.5 Å^{-1}.

for spectra collected at 100 °C, the fit having the smallest ℜ-factor resulted in a higher coordination number and a higher Debye-Waller factor. However, when the Debye-Waller factor was constrained at 0.017(Å^2), an improved fit with a coordination number having a smaller uncertainty could be obtained. The ℜ-factor did not deviate significantly from its minimum value. For data measured at 255 and 300 °C, a double shell model was required in order to obtain suitable fits. The double shell type structure is indicated by the small peak shown by arrows in Figure 5a on the right hand side of the magnitude of Fourier transform peak. The interference effects due to the presence of the double shell is also indicated in the filtered $\tilde{\chi}$(k) data (Fig. 5b) by the noticeable shift in phase with a slightly broadened oscillation (shown by arrows) relative to the other oscillations. The envelope (i.e., amplitude outline) also indicates this interference effect.

The presence of a shoulder that arises on the left hand side of the major FT peak due to noise in data, (Fig. 5a), made fitting difficult in the R-range of 1.0–3.0 Å at 255 °C. Choosing a reduced R-range of 1.4–3.0 Å facilitated the fit. Fitting done on data measured at other temperatures showed that the same filtering range would result in a significant improvement of the quality of the fits with minimal effects on the results (Table 1). When the filtering window was chosen to be 1.0–3.0 Å for the spectra measured at 300 °C, a larger ℜ-factor (0.069) was obtained indicating that the quality of the fit was not as good compared to the rest of the fits. However, use of the narrower filtering window of 1.4–3.0 Å gave a significantly improved fit with a ℜ-factor of 0.028. This resulted in fitting parameters that are quite consistent with those obtained from fitting of data measured at lower temperatures.

Having successfully fit spectra measured at 255 °C and at 300 °C using a double-shell model, the same was attempted for spectra measured at room temperature and 100 °C. How-

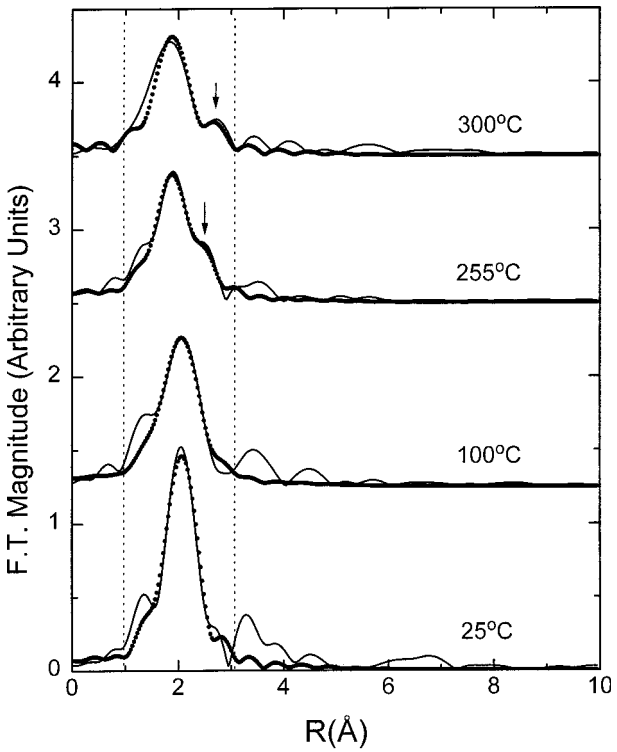

FIGURE 5(a). The magnitude of the Fourier transforms (FT, solid line) of the ($k^2\chi$) data shown in Figure 4. The 25 and 100 °C XAFS data were transformed in the k-range 2.0–8.2 Å and the 255 and 300 °C data in the k-range 2.0–8.6 Å. Fits (shown as points) to the data measured at 25, 100, and 300 °C were made in the R-range 1.0–3.0 Å. For data measured at 255 °C, the fitting was made in the R-range 1.4–3.0 Å. The arrows indicate the feature in the FT data associated with the equatorial waters of the two resolved hydration shells surrounding the La^{3+} cation.

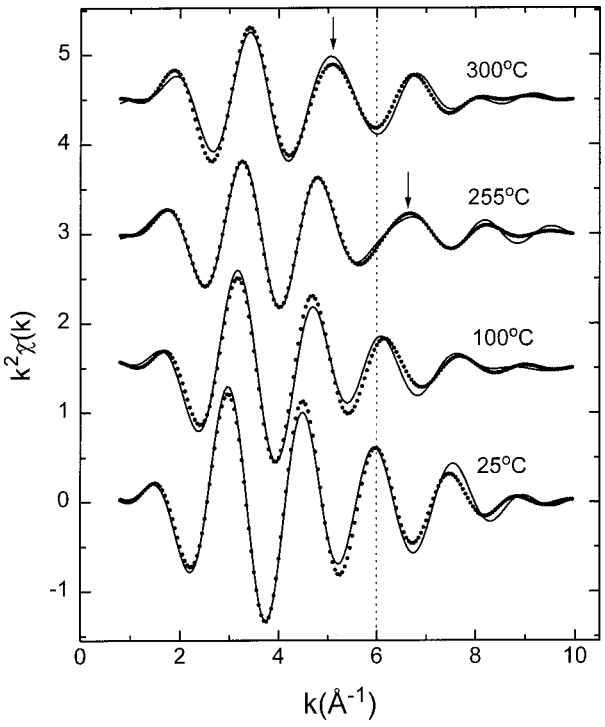

FIGURE 5(b). ($k^2\tilde{\chi}$) data filtered in the R-range 1.0–3.0 Å at 25, 100, and 300 °C and in the R-range 1.4–3.0 Å at 255 °C along with the best fit model (points) of these data. At 100 °C, $\sigma^2_{La\text{-}O}$ was constrained at 0.017 (Å^2). Note also that the dotted line going through 6.0 Å^{-1} clearly shows the change in phase of data as a function of temperature. The arrows indicate the location of the beating effect occurring due to the interference of the two resolved hydration shells surrounding the La^{3+} cation.

ever, this did not lead to physically meaningful results. Nevertheless, the possible existence of closely spaced double-shell structure in the hydration shell of La^{3+} at room temperature (Näslund et al. 2000) and at 100 °C cannot be ruled out. The relatively high Debye-Waller factor value determined from spectra measured at 100 °C may reflect large static disorder resulting from a somewhat closely spaced double-shell hydration structure surrounding the La^{3+} aqua ion.

DISCUSSION

This study is the first to describe the coordination environment of La ions in aqueous solutions at elevated temperatures. In this section we discuss our results by comparing each fitting parameter with the results from previous studies of La hydration at room temperature.

The La-OH_2 bond distance (R)

The La-OH_2 bond distance at room temperature is in good agreement with the value determined in previous XRD studies (Habenschuss and Spedding 1979b; Johansson and Wakita 1985; Kurisaki et al. 1993). Results are also consistent with the increasing bond distances from Lu to Nd reported using XAFS measurements of aqueous rare earth perchlorate solutions by Yamaguchi et al. (1988), and XAFS measurements on aqueous rare earth nitrate and chloride solutions by Yaita et al. (1999). Based on L_3-edge XAFS measurements, Solera et al. (1995) report a bond distance of 2.56 Å for La-OH_2 after removing the multielectron excitation features from the data. This result is in excellent agreement with the previous work cited above.

From their measurements on frozen solutions, Kurisaki et al. (1993) suggest that six oxygen atoms of water molecules are situated at the vertices of a trigonal prism and another three oxygen atoms lie on the equatorial plane, with all nine oxygen atoms at equal distance from the La cation. They find that the distance from the La to the equatorial oxygen atoms lengthens with increasing temperature thus giving rise to two hydration shells. It is possible that the bond length between the equatorial oxygen atoms and La begins to increase at around 100 °C as suggested by the high Debye-Waller factor (Table 1). However, the present range and quality of data measured at this temperature do not permit a double shell fit.

After further lengthening of the equatorial La-O bond lengths at 255 °C, the XAFS data reveal two separate shells of

oxygen atoms at bond distances and σ^2 values reported in Table 1. It is also interesting to note that the first shell bond distance shortens from 2.60 Å at 100 °C to 2.46 Å at 255 °C. Gorbaty and Kalinichev (1995) report a linear reduction of the degree of hydrogen bonding in water as a function of temperature over a range from 25 to about 525 °C. Estimates would give a reduction of about 30% of the amount of hydrogen bonding present at 255 °C compared to that at room temperature. It is possible that the weakening or breaking of the hydrogen bonds between the second- and first-shell hydration waters at this temperature results in the attraction of the non-equatorial oxygen atoms toward the cation which in turn drives the weaker equatorial oxygen atoms outward to maintain the dipole electrostatic equilibrium. At 300 °C the equatorial bonds are even longer (2.79 Å). The reverse of the above is also possible. That is, in order to preserve equilibrium, the first shell oxygen atoms move closer to the lanthanide cation (through the breakage of hydrogen bonding) as a result of stretching out of oxygen atoms in the second shell due to their temperature dependent nature.

The coordination number (N)

The hydration number for La^{3+} ion in aqueous solutions is reported to be nine. (e.g., Habenschuss and Spedding 1979b; Kurisaki et al. 1993; Kanno and Hiraishi 1984). This result is also consistent with XAFS (e.g., Allen et al. 2000; Yamaguchi et al. 1988; Yaita et al. 1999) and neutron diffraction (Helm et al. 1994) measurements made on aqueous light REE-bearing solutions. Taking into consideration the uncertainty of the coordination number (i.e., approximately 7–15% in the single shell fits and 17–25% in the double shell fit), our results are in very good agreement with previously reported coordination number of nine. The coordination number at 100 °C is the same as at room temperature. Our analyses show that the total coordination number at 255 and 300 °C remains close to nine while maintaining a non-equatorial to equatorial oxygen ratio of approximately 2:1.

Solera et al. (1995) reported a coordination number of 12 for all the lanthanides irrespective of their atomic number. It is possible that this discrepancy is due to the use of a low S_0^2 value for lanthanides (e.g., Stern 1988) in their theoretical estimation. The S_0^2 value used in their analysis is not reported. More accurate values of S_0^2 that are currently available are in the order of 25 to 30% larger than the values used by Solera et al. (1995). Zhu et al. (1993) also reported a 12-coordinated La^{3+} ion, based on the X-ray crystallographic measurements made on a crystalline lanthanum compound.

The XAFS Debye-Waller factor (σ^2)

The room temperature Debye-Waller factor reported in this study is in good agreement with that reported by Solera et al. (1995). It is also consistent with the increasing change in Debye-Waller factors from Lu to Nd reported by Yamaguchi et al. (1988). Estimates based on Ln-O vibrational frequency Raman data reported by Kanno and Hiraishi (1984) would give rise to a σ_{vib}^2 value of 0.0048 (Å^2) at room temperature. The XAFS Debye-Waller factor therefore, being an overall representation given by $\sigma^2 = \sigma_{stat}^2 + \sigma_{vib}^2$ where σ_{stat}^2 and σ_{vib}^2 are contributions due to the static disorder and thermal vibrations respectively, would account for the reported value in our work. The high σ^2 at 100 °C may be a result of increased static disorder (higher σ_{stat}^2) that arises due to the initial increase in bond length between the equatorial O atoms and lanthanum as discussed above. The reduction of the Debye-Waller factors at 255 and 300 °C is primarily due to a large reduction of static disorder in each of the separate oxygen shells. These results provide a basis for future XAFS investigations of the association of REEs by ligands such as Cl^-, F^-, OH^-, CO_3^{2-}, SO_4^{2-}, and PO_4^{3-} in more chemically complex natural systems. In addition, this study demonstrates the utility of the modified hydrothermal diamond anvil cell as a tool for relatively low energy X-ray spectroscopic investigations of dilute fluids at elevated temperatures and pressures.

ACKNOWLEDGMENTS

We thank S. Heald and other PNC-CAT beam line personnel and R. Gordon of Simon Fraser University for assisting with our experiments at the Advanced Photon Source. This research was funded by a Natural Sciences and Engineering Research Council of Canada (NSERC) research and equipment grant to A.J.A. and a grant from the Research Corporation to R.A.M. NSERC is also thanked for providing funds for this project through a Major Facility Access Grant. The U.S. Department of Energy, Basic Energy Sciences, Office of Science, under contract no. W-31-109-Eng-38 (APS) and DE-FG03-97ER45628 (PNC-CAT) supported the use of the Advanced Photon Source. Finally, we thank H.W. Nesbitt and two reviewers for their constructive suggestions.

REFERENCES CITED

Allen, P.G., Butcher, J.J., Shuh, D.K., Edelstein, N.M., and Creig, I. (2000) Coordination chemistry of trivalent lanthanide and actinide ion in dilute and concentrated chloride solutions. Journal of Inorganic Chemistry, 39, 595–601.

Anderson, A.J., Mayanovic, R.A., Chou, I-M., and Bassett, W.A. (2000) XAFS investigations of zinc halide complexes up to supercritical conditions. In P.R. Tremaine, P.G. Hill, D.E. Irish and P.V. Balakrishnan, Eds., Steam, Water and Hydrothermal Systems: Physics and Chemistry meeting the Needs of Industry. Proceedings of the 13th International Conference on the Properties of Water and Steam, NCR Press Ottawa.

Bassett, W.A., Anderson, A.J., Mayanovic, R.A., and Chou, I-M. (2000a) Hydrothermal diamond anvil cell XAFS studies of first-row transition elements in aqueous solutions up to supercritical conditions. Chemical Geology, 167, 3–10.

———(2000b) Modified hydrothermal diamond anvil cells for XAFS analyses of elements with low energy absorption edges in aqueous solutions at sub- and supercritical conditions. Zeitschrift für Kristallographie, 215, 711–717.

Brookins, D.G. (1989) Aqueous Geochemistry of Rare Earth Elements. In B.R. Lipin and G.A. McKay, Eds., Geochemistry and mineralogy of rare earth elements, 21, 201–223. Reviews in Mineralogy, Mineralogical Society of America, Washington, D.C.

Fulton, J.L., Pfund, D.M., Wallen, S.L., Newville, M., Stern, E.A., and Ma, Y. (1996) Rubidium ion hydration in ambient and supercritical water. Journal of Physical Chemistry, 105, 2161–2166.

Gammons, C.H. and Wood, S.A. (2000) The aqueous geochemistry of REE. Part 8: Solubility of ytterbium oxalate and the stability of Yb(III)-oxalate complexes in water at 25 °C to 80 °C. Chemical Geology, 166, 103–124.

Gorbaty, Y. E. and Kalinichev, A. G. (1995) Hydrogen bonding in supercritical water. 1. experimental results, Journal of Physical Chemistry, 99, 5336–5340.

Haas, J.R., Shock, E.L., and Sassani, D.C. (1995) Rare earth elements in hydrothermal systems: Estimates of standard partial molal thermodynamic properties of aqueous complexes of the rare earth elements at high pressures and temperatures, Geochimica et Cosmochimica Acta, 59, 4329–4350.

Habenschuss, A. and Spedding, F.H. (1979a) The coordination (hydration) of rare earth ions in aqueous chloride solutions from X-ray diffraction. I. $TbCl_3$, $DyCl_3$, $ErCl_3$, $TmCl_3$, and $LuCl_3$. Journal of Physical Chemistry, 70, 2797–2805.

———(1979b) The coordination (hydration) of rare earth ions in aqueous chloride solutions from X-ray diffraction. II. $LaCl_3$, $PrCl_3$, and $NdCl_3$. Journal of Physical Chemistry, 70, 3758–3763.

Haskel, D., Stern, E. A., Dogan, F., and Moodenbaugh, A.R. (2000) XAFS study of the low-temperature tetragonal phase of $La_{2-x}Ba_xCuO_4$: Disorder, stripes, and T_c suppression at x = 0.125. Physical Review B, 61, 7055–7076.

Helm, L., Foglia, F., Kowall, T., and Merbach, A. (1994) Structure and dynamics of lanthanide ions and lanthanide complexes in solution. Journal of Physics, 6, A137–A140.

Hoffmann, M.M., Darab, J.G., Heald, S.M., Yonker, C.R., and Fulton, J.L. (2000)

New experimental developments for in situ XAFS studies of chemical reactions under hydrothermal conditions. Chemical Geology, 167, 89–103.

Johansson, G. and Wakita. H. (1985) X-ray investigation of the coordination and complex formation of lanthanoid ions in aqueous perchlorate and selenate solutions. Journal of Inorganic Chemistry, 24, 3047–3052.

Kanno, H. and Hiraishi, J. (1984) Raman study of aqueous rare-earth nitrate solutions in liquid and glassy states. Journal of Physical Chemistry, 88, 2787– 2792.

Krauskopf, K.B. (1986) Thorium and rare-earth metals as analogs for actinide elements. Chemical Geology, 55, 323–335.

Kurisaki, T., Yamaguchi, T., and Wakita, H. (1993) Effects of temperature on the structure of hydrated lanthanide (III) ions in crystals and in solution. Journal of Alloys and Compounds, 192, 293–295.

Lewis, A.J., Komninou, A., Yardley, B.W.D., and Palmer, M.R. (1998) Rare earth element speciation in geothermal fluids from Yellowstone National Park, Wyoming, USA, Geochimica et Cosmochimica Acta, 62, 657–663.

Mayanovic, R.A., Anderson, A.J., Bassett, W.A., and Chou, I.M. (1999) XAFS measurements on zinc chloride aqueous solutions from ambient to supercritical conditions using the diamond anvil cell. Journal of Synchrotron Radiation, 6, 195–197.

Mosselmans, J.F.W., Schofield, P.F., Charnock, J.M., Garner, C.D., Pattrick, R.A.D., and Vaughan, D.J. (1996) X-ray absorption studies of metal complexes in aqueous solution at elevated temperatures. Chemical Geology, 127, 339–350.

Näslund, J., Lindqvist-Reis, P., Persson, I., and Sandström, M. (2000) Steric Effects Control the Structure of the Solvated Lanthanum(III) Ion in Aqueous, Dimethyl Sulfoxide, and *N,N′*-Dimethylpropyleneurea Solution. An EXAFS and Large-Angle X-ray Scattering Study. Journal of Inorganic Chemistry, 39, 4006–4011.

Newville, M., Livins, P., Yacoby, Y., Rehr, J., and Stern, E.A. (1993) Near-edge X-ray absorption fine structure of Pb: A comparison of Theory & Experiment. Physical Review B, 47, 14126–14131.

Newville, M., Ravel, B., Haskel, D., Rehr, J.J., Stern, E.A., and Yacoby, Y. (1995) Analysis of multiple-scattering XAFS data using theoretical standards. Physical Review B, 208 & 209, 154–156.

Oelkers, E.H., Sherman, D.M., Ragnarsdottir, K.V., and Collins, C. (1998) An EXAFS spectroscopic study of aqueous antimony(III)-chloride complexation at temperatures from 25 °C to 250 °C. Chemical Geology, 151, 21–27.

Ragnarsdottir, K.V., Oelkers, E.H., Sherman, D.M., and Collins, C.R. (1998) Aqueous speciation of yttrium at temperatures from 25 to 340 °C at P_{sat}: an in situ EXAFS study. Chemical Geology, 151, 29–39.

Sayers, D.E. and Bunker, B.A. (1988) Data Analysis. In D.C. Koningsberger and R. Prins, Eds., X-ray Absorption: Principles, Applications, Techniques of EXAFS, SEXAFS and XANES, p. 211–253. Wiley, New York.

Seward, T.M. and Barnes, H.L. (1997) Metal transport in hydrothermal ore fluids. In H.L. Barnes, Ed., Geochemistry of Hydrothermal Ore Deposits, 3rd ed., p. 435–486. Wiley, New York.

Seward, T.M., Henderson, C.M.B., Charnock, J.M., and Driesner, T. (1999) An EXAFS study of solvation and ion pairing in aqueous strontium solutions to 300 °C. Geochimica et Cosmochimica Acta, 63, 2409–2418.

Sherman, D.M., Ragnarsdottir, K.V., Oelkers, E.H., and Collins, C.R. (2000) Speciation of tin (Sn^{2+} and Sn^{4+}) in aqueous Cl solutions from 25 °C to 350 °C: an in situ EXAFS study. Chemical Geology, 167, 169–176.

Solera, J.A., Garcia, J., and Proietti, M.G. (1995) Multielectron excitations at the L edges in rare-earth ionic aqueous solutions. Physical Review B, 51, p. 2678–2686.

Stern, E.A. (1988) Theory of EXAFS. In D.C. Koningsberger and R. Prins, Eds., X-ray Absorption: Principles, Applications, Techniques of EXAFS, SEXAFS and XANES, p. 3–51. Wiley, New York.

Stern, E.A., Newville, M., Ravel, B., Yacoby, Y., and Haskel, D. (1995) UWXAFS analysis package: Philosophy and Details. Physical Review B, 208 & 209, 117–120.

Taylor, R.P. and Fryer, B.J. (1982) Rare Earth Element Geochemistry as an Aid to Interpreting Hydrothermal Ore Deposits. In A.M. Evans, Ed., Metallization Associated with Acid Magmatism, 6, 357–365. Wiley, New York.

Williams-Jones, A.E., Samson, I.M., and Olivo, G.R. (2000) The genesis of hydrothermal fluorite-REE deposits in the Gallinas Mountains, New Mexico. Economic Geology, 95, 327–342.

Wood, S.A. (1990) The aqueous geochemistry of the rare earth elements and yttrium: Part II. Theoretical predictions of speciation in hydrothermal solutions to 350 °C at saturated water vapor pressure. Chemical Geology, 88, 99–125.

Wood, S.A., Tait, C.D., Janecky, D.R., and Constantopoulos, T.L. (1995) The aqueous geochemistry of rare earth elements: V. Application of photoacoustic spectroscopy to speciation at low rare earth element concentrations. Geochemica et Cosmochimica Acta, 59, 5219–5222.

Yaita, T., Narita, H., Suzuki, Sh., Tachimori, Sh., Motohashi, H., and Shiwaku, H. (1999) Structural study of lanthanides (III) in aqueous nitrate and chloride solutions by EXAFS. Journal of Radioanalytical and Nuclear Chemistry, 239, 371–375.

Yamaguchi, T., Nomura, M., Wakita, H., and Ohtaki, H. (1988) An extended X-ray absorption fine structure study of aqueous rare earth perchlorate solutions in liquid and glassy states. Journal of Chemical Physics, 89, 5153–5159.

Zabinsky, S.I., Rehr, J.J., Ankudinov, A., Albers, R.C., and Eller, M.J. (1995) Multiple-scattering calculations of X-ray spectra. Physical Review B, 52, 2995–3009.

Zhu, Y., Liu, W.S., Tan, M., Jiao, T., and Tan, G. (1993) X-ray crystal structure of the 1:1 complex between lanthanum nitrate and N,N,N',N'-tetraphenyl-3,6-Dioxaoctanedioic Diamide. Polyhedron,12, 939–944.

MANUSCRIPT RECEIVED OCTOBER 13, 2000
MANUSCRIPT ACCEPTED NOVEMBER 5, 2001
MANUSCRIPT HANDLED BY H.W. NESBITT